
This is an electronic reprint of the original article.
This reprint may differ from the original in pagination and typographic detail.

Heldmann, Janis; Cucharero, Jose; Lokki, Tapio

Sound absorption of foam-formed softwood fibers: Characterization, modeling, prediction

Published in:
Applied Acoustics

DOI:
[10.1016/j.apacoust.2025.111200](https://doi.org/10.1016/j.apacoust.2025.111200)

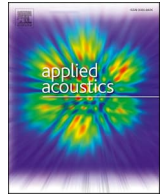
Published: 01/03/2026

Document Version
Publisher's PDF, also known as Version of record

Published under the following license:
CC BY

Please cite the original version:
Heldmann, J., Cucharero, J., & Lokki, T. (2026). Sound absorption of foam-formed softwood fibers: Characterization, modeling, prediction. *Applied Acoustics*, 245, Article 111200.
<https://doi.org/10.1016/j.apacoust.2025.111200>

This material is protected by copyright and other intellectual property rights, and duplication or sale of all or part of any of the repository collections is not permitted, except that material may be duplicated by you for your research use or educational purposes in electronic or print form. You must obtain permission for any other use. Electronic or print copies may not be offered, whether for sale or otherwise to anyone who is not an authorised user.



Sound absorption of foam-formed softwood fibers: Characterization, modeling, prediction

Janis Heldmann^{a,*} , Jose Cucharero^b, Tapio Lokki^a 

^a Acoustics Lab, Aalto University, Department of Information and Communications Engineering, Otakaari 5A, Espoo, 02150, Finland

^b Lumir Oy, Linjatie 2, Vantaa, 01260, Finland

HIGHLIGHTS

- Hybrid JCAL analytical model refined via fitting to non-acoustic parameters for better absorption predictions.
- Foam-formed softwood fiber foams tuned across 19–64 kg/m³; absorption maxima shift systematically with density.
- JCAL/JCA/JCAL–Biot compared to measurements; JCAL–Biot captures elastic effects in high-density samples.
- Sample fitting/compression affects estimated flow resistivity and elastic resonances, highlighting setup sensitivity.

ARTICLE INFO

Keywords:

Bio-based materials
Analytical modeling
Foam-forming
Wood fibers

ABSTRACT

In contemporary society, the urgent need to transition to building materials with low or negative carbon dioxide footprints is driven by increasing environmental concerns. Therefore, bio-based materials draw increasing attention in research literature, especially when utilized as thermal and acoustic insulation. Traditional materials predominantly used as acoustic materials, such as mineral wools, incur substantial energy consumption during production, primarily through the melting of sand. In contrast, bio-based materials offer promising alternatives to current market leaders potentially achieving negative carbon footprints due to their low embodied energy and high carbon content. When sourced from industrial by-products, these materials have the ability to store carbon in buildings for decades. It is crucial to investigate the porous structures of these bio-fibrous materials to unlock their full potential. Therefore, this study focuses on the prediction and characterization of foam-formed softwood-based fibers and their acoustic properties. By evaluating analytical models, semi-phenomenological models, and experimental measurements, the prediction of sound absorption based on fiber diameter and density is assessed. Moreover, the material synthesis process and characterization are adapted to achieve a wider range of densities while taking elastic properties into account. The findings reveal that refining a recent analytical model for natural fibers through parameter fitting to non-acoustic parameters yields improved accuracy in predicting sound absorption curves. This work lays the groundwork to create environmentally sustainable sound absorbers with carefully tailored sound absorption properties.

1. Introduction

In recent years, there has been a significant increase in attention toward stress-related illnesses caused by noise and sound pollution. Noise exposure can lead to various health issues such as sleep disturbances, hearing loss, hypertension, and lack of focus [1]. Reducing noise through acoustic strategies can alleviate stress and improve performance for students and teachers in schools, speed up recovery in hospitals, and enhance productivity while reducing stress in offices [2–7]. Moreover, good acoustic design enhances the quality of life and creates more enjoyable

environments, such as in restaurants [8]. A common approach to minimizing unwanted noise and improving room acoustics is the use of sound-absorbing materials [9]. Among different options, porous materials are often favored over resonant absorbers due to their broad frequency range. Fibrous materials, in particular, are known to effectively dissipate energy because of their intricate microstructure [10,11].

The selection of materials for sound absorbers is influenced not only by their performance but also by their environmental impact. The construction industry is responsible for approximately one-third of global carbon dioxide emissions, making it essential for society to shift toward

* Corresponding author.

Email address: janis.heldmann@aalto.fi (J. Heldmann).

carbon neutrality by using building materials with neutral or, preferably, negative carbon footprints. Common sound-absorbing materials include mineral wools like glass wool or rock wool, which require significant energy for production as they involve melting glass or stone in large furnaces and spinning the molten material into a wool structure [12]. However, environmentally sustainable alternatives do exist and carry the potential to replace glass and rock wool while achieving comparable or even better sound attenuation, e.g., in the form of bio-based sound absorbers [13,14].

In the past decade, numerous bio-based materials have been explored as potential substitutes for mineral wools. These include various materials made with natural fibers like coir [15], date palm [16–18], hemp [19], kenaf [20], yucca gloriosa [21], and nettle [22], as well as recycled fibers such as wood, textile waste [23,24], polypropylene [25], and cellulose acetate fibers [26]. While many of these materials exhibit good sound absorption properties, they are often raw materials that require further processing to be suitable for use as building materials. A recent study showed that processed foam-formed wood-based fibers had sound absorption characteristics similar to mineral wool, highlighting their potential as a sustainable alternative in construction [27]. Wood as a base material acts during its lifecycle as a natural carbon sink [28,29]. When the carbon footprint of the processed material is lower than the carbon stored in the base material, the sustainable absorbers becomes carbon negative. During foam-forming, the material is merely stirred and air-dried leading to low embodied energy in the end-product. A related LCA study was conducted by Lumir Oy [30].

Wood-based materials offer several benefits, including low carbon footprints and availability as byproducts of the pulp and paper industry. These materials are typically made from wood chips [31], processed pulp [27], or a combination of both [32]. They can be derived from bleached or dissolving hardwood and softwood pulps. A key factor in sound absorption is the method used to create a porous structure, as this impacts the material's microstructure. Generally, the fibrous composition of wood-based materials is highly effective for sound absorption due to the viscous and thermal interactions between the fluid and solid fibers.

1.1. Modelling of sound absorption properties

Various models are available to describe the acoustic performance of porous fibrous materials, utilizing empirical, numerical, analytical, or semi-phenomenological approaches. Empirical models are based on extensive measurement data to determine the parameters governing sound absorption. Numerical models, such as those using finite-element methods, simulate and calculate these parameters. Analytical models provide simplified equations, often derived from physical principles, and are validated through numerical models. Semi-phenomenological models combine empirical relationships between observed phenomena and physical parameters. Generally, as the complexity of the pore or fiber structure being modeled increases, so does the complexity and number of parameters in the model.

A simple model for estimating the acoustic performance of porous materials, based solely on flow resistivity, was developed by Delany and Bazley in 1970 [33]. Zwicker and Kosten's model, which describes numerous cylindrical tubes, uses flow resistivity and open porosity for its calculations. By incorporating the high-frequency limit of tortuosity, their model was extended to account for slanted cylindrical pores. Further refinement, assuming non-uniform pore diameters along the pore direction, led to models that consider both the minimum and maximum pore diameters. Currently, the most widely used model is the Johnson-Champoux-Allard-Lafarge (JCAL) model, a well-established semi-phenomenological approach. It calculates the absorption curve of a porous material based on six non-acoustic parameters: open porosity, flow resistivity, tortuosity, viscous and thermal characteristic lengths, and thermal permeability. Extended into the JCAL-Biot model, the elastic properties of the rigid frame are also taken into account.

Characterization of the non-acoustic parameters usually involves both measurement and estimation. Flow resistivity can be directly measured, and porosity can be estimated if the bulk and fiber densities of the material are known. Tortuosity can be measured via ultrasound methods but can also be derived from porosity. The remaining parameters thermal permeability, viscous characteristic length, and thermal characteristic length rely on numerical inversion. By using a three-microphone impedance tube, the material's dynamic bulk modulus \tilde{K} and dynamic density $\tilde{\rho}$ are measured, and the parameters are then adjusted to their real and complex components to derive the non-acoustic parameters for the JCAL model. Additionally, a recent study suggests that porosity can be estimated from airflow resistivity, simplifying the experimental process to measuring flow resistivity and determining the dynamic bulk modulus and dynamic density. Eventually, even airflow resistivity can be estimated by combining the measured sound absorption spectrum, dynamic bulk modulus and dynamic density [34].

Predicting sound absorption before material production typically requires finite element method (FEM) simulations with appropriate 3D models, which can be quite challenging [35]. In contrast, accurate analytical models offer the ability to predict sound absorption behavior using parameters known or selected prior to material synthesis. Some analytical models enable the prediction of acoustic absorption based solely on fiber geometry and bulk density. This approach's key advantage is that, once the fiber geometry of the base material has been determined, no extensive measurements are required; the desired effective density can simply be chosen during the synthesis process.

Analytical models can be grouped into three main categories. The first relies on empirical relationships derived from regression analysis of experimental data. The second category builds models based on a detailed understanding of fibers spatial distribution, including factors such as fiber orientation and radii. The third category combines measured density data with an analytical framework to compute non-acoustic parameters across varying densities.

These models generally make certain assumptions about fiber geometry and spatial arrangement. For example, natural fibers often exhibit random spatial distributions and a non-uniform, symmetric spread of diameters, in contrast to the more uniform properties typically seen in synthetic fibers. A recent study by Pompoli et al. (2023) demonstrated the success of integrating a hybrid JCAL approach with a numerical model for analyzing natural *Posidonia* fibers, achieving highly accurate results [36].

In this study, a straightforward hybrid analytical model is assessed and refined to more precisely predict the sound absorption curves of foam-formed softwood fibers at various densities and specified fiber radii. To the authors' knowledge, this hybrid JCAL method and its extension to any density using an analytical model for foam-formed wood fibers have not been explored in previous research. The findings are compared with experimental data and the simulated absorption derived from the characterized JCAL and JCA parameters.

2. Materials and methods

2.1. Materials

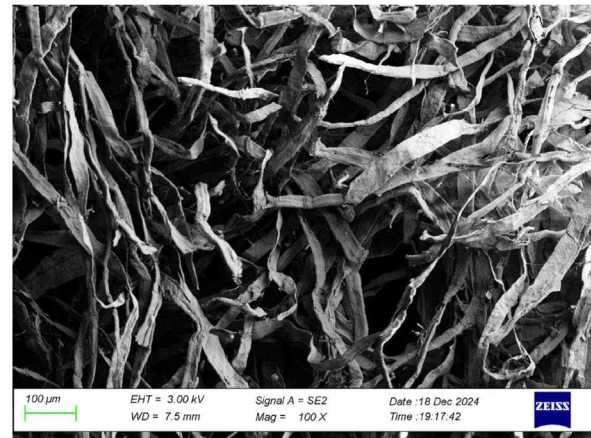
The materials examined in this research are wood-based fibrous structures created through a foam-forming method [37]. The base material is a bleached softwood pulp sourced from Finnish biorefineries. Various types of pulps differ in terms of fiber count per volume, as well as fiber diameter and length. Generally, softwood pulps feature longer fibers with larger diameters compared to, e.g., hardwood pulps [27].

2.2. Preparation of samples

Foams designed for sound absorption were produced using a foam-forming process as outlined in [27]. This technique involved mixing pulp, water, and sodium dodecyl sulfate (SDS) while applying axial agitation at about 3000 rpm in a cylindrical vessel measuring 40 cm in



(a) Material



(b) Scanning electron microscopy image

Fig. 1. Studied material made out of softwood fibers with foam-forming technique, showing (a) foam sample and (b) a scanning electron microscopy image showing the fibrous network.

length and 24 cm in diameter. Different pulp consistencies (1 % and 3.5 %) were used to create foams with varying densities. The SDS dosage was consistently maintained at 0.5 g/L up to 59 kg/m³. The dry pulps were first soaked in 5 liters of tap water at room temperature for one day. Before adding SDS, the pulp-water mixture was stirred for 10 minutes to ensure even dispersion of the fibers. After introducing the SDS, the mixture was foamed until its volume doubled.

The resulting fiber foam was poured into a cubic mold (25 cm × 25 cm × 25 cm) with two stainless steel nets at the bottom. Gravity drainage was allowed for over 15 minutes, with the top net featuring a mesh size of 0.16 mm and the bottom net having a 5 mm opening to support the sample and prevent deformation. The foams were then dried in a drying cabinet at 40 °C for two days. For the denser foams, a small amount of water was sprayed on the samples, which were then placed in a sealed container at 99 % relative humidity and 20 °C for two days. After conditioning, the samples were compressed to a thickness of 45 mm and dried in the cabinet for one day while maintaining compression. Circular samples were subsequently extracted from the foam using a bench drill, resulting in varied inner densities, with greater density at the base. To ensure uniform density, layers of fiber foam were carefully removed from both sides until a thickness of 40 mm was reached. Fig. 1 shows a foam sample and a SEM image showing the fibrous network. The diameters of the foam samples were standardized to 100 mm for sound absorption and flow resistivity measurements. For densities above 45 kg/m³, the foams collapsed during the drying process. Therefore, SDS was replaced with a non-ionic surfactant which affected the fiber-to-fiber interaction and stabilized the fibrous network. The pulp consistencies were then increased up to 4.5 %. Additionally, three samples were created with a diameter of 29 mm to allow a broader frequency range of investigation in the impedance tube.

2.3. Measurement of normal incidence sound absorption, dynamic bulk modulus and dynamic mass density

The acoustic effective properties ($\tilde{\rho}$ and \tilde{K}) were measured using the three-microphone technique within a 100-mm diameter B&K 4206 impedance tube. A broad-spectrum random signal ranging from 50 Hz to 2000 Hz was generated by a loudspeaker located at one end of the tube. The samples were placed at the end of the standing wave tube, which had a rigid termination. Microphones 1 and 2 were positioned at standard distances of 50 mm and 100 mm, respectively, while microphone 3 was flush-mounted on the 3D-printed rigid end. The frequency-dependent parameters were determined in accordance with ISO-10534-2 [38]. Each material sample was measured on both

sides, as this approach is effective for potentially non-homogeneous bio-materials. The results reported are averages of the values obtained from both sides of a single sample. Additionally, the 29 mm samples were measured in the smaller diameter setup of the impedance tube allowing for investigation in the range of 50 – 5000 Hz. The change in tube diameter was necessary to cover a wider frequency range because the cut-off frequency of an impedance tube depends on its internal diameter. Below the first non-plane mode cut-off frequency, the sound field inside the tube can be assumed to be plane, which is a prerequisite for the validity of the transfer-matrix method used to determine the acoustic properties. A smaller tube supports plane-wave propagation up to higher frequencies, while a larger tube allows accurate measurements at lower frequencies due to the larger cross-sectional area and reduced influence of viscous and thermal boundary layers.

2.4. Measurement of flow resistivity

A measurement apparatus was developed following ISO standard 9053-1:2018 to evaluate the airflow resistivity of the pulp fiber foams. Differential pressure across the samples was measured using a differential pressure meter (MIRAN DP-200, Pietiko Oy, Finland), while a constant airflow was maintained with the help of an air compressor. Flow regulation was achieved through an airflow regulator, adjusting the volumetric flow to a range of 3–6 l/m³ (Mass flow meter Red-y Compact, Votglin, Switzerland). Airflow resistivity was calculated using Eq. (1), where Δp represents the differential pressure across the sample, A is the cross-sectional area of the specimen, q_v is the constant volumetric airflow through the sample, and d indicates the thickness of the sample. Measurements of airflow resistivity were performed on the foams made from softwood pulp, with samples of similar densities averaged for the results.

$$\sigma = \frac{\Delta p * A}{q_v * d} \quad (1)$$

2.5. Characterization with JCAL and JCA models

The JCAL model is a semi-phenomenological framework that utilizes six non-acoustic parameters to describe sound dissipation. These parameters address sound dissipation caused by viscous effects, represented by the high-frequency limit of tortuosity (α_∞) and the viscous characteristic length (Λ), as well as thermal effects, characterized by the thermal characteristic length (Λ') and thermal permeability (k'_0). Additionally, the model incorporates porosity (ϕ), which is the ratio of open pore volume to total volume, and airflow resistivity (σ), both of which contribute

to dissipation in thermal and viscous domains. The model is founded on the principle that dynamic density ($\tilde{\rho}$) and dynamic bulk modulus (\tilde{K}) can be expressed through these six non-acoustic parameters.

$$\tilde{\rho}(\omega) = \frac{\alpha_{\infty}\rho_0}{\phi} \left[1 + \frac{\sigma\phi}{j\omega\rho_0\alpha_{\infty}} \sqrt{1 + j \frac{4\alpha_{\infty}^2\eta\rho_0\omega}{\sigma^2\Lambda^2\phi^2}} \right] \quad (2)$$

$$\tilde{K}(\omega) = \frac{\gamma P_0/\phi}{\gamma - (\gamma - 1) \left[1 - j \frac{\phi\kappa}{k'_0 C_p \rho_0 \omega} \sqrt{1 + j \frac{4k'_0{}^2 C_p \rho_0 \omega}{\kappa \Lambda'^2 \phi^2}} \right]} \quad (3)$$

The absorption coefficient can be determined by calculating the surface impedance using the values of $\tilde{\rho}$ and \tilde{K} . The JCA model expresses the dynamic bulk modulus without accounting for thermal permeability, which places greater emphasis on viscous effects. The JCAL-Biot model also takes into account the elastic properties of the solid material into account. These effects are usually more relevant when the samples have been compressed during fitting into the impedance tube. Additionally, once $\tilde{\rho}$ and \tilde{K} are experimentally obtained, the non-acoustic properties are derived using the indirect method proposed by Panneton and Olny. This method involves analytical solutions from the viscous model by Johnson et al. and the thermal model by Lafarge et al. In this study, the software RokCell is utilized to estimate flow resistivity tortuosity, viscous and thermal characteristic lengths, and thermal permeability by minimizing the error in the normal incidence sound absorption based on $\tilde{\rho}$ and \tilde{K} . Airflow resistivity has been first obtained from direct measurement. However, fitting the sample into the flow meter, can lead to inaccurate values if the sample sits too tightly or too loosely. In this study, measured flow resistivity was too high compared to estimated results suggesting tight fitting. Therefore, the investigation proceeded with the estimated values. Further, porosity is calculated based on bulk density (ρ) and fiber density. Since cellulose constitutes the majority of the fiber content, fiber density is estimated at $\rho_f = 1500 \text{ kg/m}^3$, leading to the porosity equation:

$$\phi = 1 - \frac{\rho}{\rho_f} \quad (4)$$

For those samples with elastic effects present in the measured absorption curve, the Young's modulus E , Poisson's ratio ν , and loss-factor η_e were estimated while fitting the JCAL-Biot model to the absorption curve. However, these estimations are not validated by experimental measurement and therefore lack robustness in predicting absorption behavior under for example different rates of compression or coupling to a rigid frame. Therefore, a selection of samples has been compressed to fit less tightly into the impedance tube with the aim of reducing the impact of elastic properties in measurement and prediction. The results are briefly described in Section 3.4.

2.6. Prediction with analytical models

The analytical model used in this study is based on the premise of randomly oriented parallel fibers with a symmetric distribution of radii, as outlined in [36]. This approach is particularly suitable for bio-based materials that naturally form, unlike synthetic fibers. The model relies on the effective radius a and bulk density ρ , with the density calculated by weighing the samples and dividing by the volume of their enclosing frame. The densities of all samples are presented in Table 1. The effective radius $a = 12.7 \mu\text{m}$ for softwood was determined by a Kajaani FiberLab optical fiber analyser (Metso automation, Finland) in a previous study on foam-formed fibers from the same source [39]. The analytical model derives non-acoustic parameters using a series of equations adapted from various authors to suit symmetric radii distributions with respect to their fitting coefficients.

Table 1

Softwood samples with averaged values for density ranges of produced foam-formed cellulose samples. Sample diameter: 100 mm (except samples 19–20 with 29 mm). Sample height: 400 mm. The mean fiber diameter is $1.04 \times 10^{-5} \text{ mm}$ for softwood fibers [27]. The * marks samples with substituted non-ionic surfactant and ** marks samples with reduced diameter.

Softwood (SW)		
	Weight (g)	Density (kg/m ³)
1	5.7	18.1
2	6.1	19.4
3	6.2	19.7
4	6.4	20.4
Avg. 1	6.1	19
5	8.1	25.8
6	8.2	26.1
7	9.2	29.3
8	9.5	30.2
9	9.5	30.2
10	10.0	31.8
Avg. 2	9.1	29
11	13.6	43.3
12	14.0	44.6
13	15.1	48.1
14	15.6	49.7
Avg. 3	14.8	46
15*	16.0	50.0
16*	17.0	53.0
17*	18.0	56.0
18*	20.0	59.0
19**	1.5	59.0
20**	1.7	64.0

For the model, airflow resistivity is calculated according to Tamayol et al. [40] using the formula:

$$\sigma = \frac{\eta}{(2a)^2} c_1 \frac{\sqrt{1 - (1 - \phi)}}{\left(\frac{c_2}{1 - \phi} - 3 \sqrt{\frac{c_2}{1 - \phi}} + 3 - \sqrt{\frac{1 - \phi}{c_2}} \right)} \quad (5)$$

where a is the effective fiber radius and η is the viscosity of air. The fitting parameters $c_1 = 0.21$ and $c_2 = 0.71$ are specifically for symmetric distributions of parallel fibers.

Tortuosity is calculated using Archi's Law [41] with a fitting coefficient of 0.9574:

$$\alpha_{\infty} = \left(\frac{1}{\phi} \right)^{0.9574} \quad (6)$$

The viscous characteristic length is determined by the model of Umnova et al. [42] as follows:

$$\Lambda = a \frac{(2 - \phi)\phi^{2.732}}{2(1 - \phi)} \quad (7)$$

The model of Luu et al. [43] is modified to:

$$\Lambda' = a \frac{\phi}{(1 - \phi + 0.0023)} \quad (8)$$

Static thermal permeability is determined using Umnova et al.'s model [42]:

$$k'_0 = a^2 \frac{3.107\eta}{\sigma \cdot \phi^{2.506}} \quad (9)$$

where σ represents air flow resistivity. In this study, the prediction of the sound absorption curve for foam-formed softwood fibers begins with the aforementioned model. The model is further refined by fitting air

Table 2
Results for the characterization of acoustic and elastic parameters of all samples in RokCell software.

(a) Acoustic and structural parameters estimated in RokCell.						
Density (kg/m ³)	σ (Nsm ⁻⁴)	ϕ (-)	α_∞ (-)	Λ (μ m)	Λ' (μ m)	k'0 (1e-10 m ²)
19	5900 (1300)	0.99 (0)	1.04 (0.03)	65 (6)	140 (13)	59 (11)
29	11,800 (1600)	0.98 (0)	1.05 (0.04)	45 (4)	107 (20)	32 (9)
46	19,600 (1300)	0.97 (0)	1.04 (0.05)	21 (3)	110 (13)	14 (2)
50	37,600 (1800)	0.97 (0)	1.1 (0.1)	24 (1)	247 (23)	32 (10)
53	47,600 (8100)	0.97 (0)	1.1 (0.12)	22 (8)	217 (39)	40 (5)
56	50,200 (1600)	0.97 (0)	1.19 (0.15)	25 (13)	191 (19)	42 (19)
59	50,400 (7700)	0.97 (0)	1.11 (0.14)	24 (12)	146 (20)	52 (6)
59	60,000 (3100)	0.97 (0)	1.17 (0.08)	28 (4)	108 (32)	12 (2)
64	73,200 (5700)	0.97 (0)	1.08 (0.09)	27 (4)	78 (15)	16 (17)

(b) Sample diameter and elastic parameters from RokCell.					
Density (kg/m ³)	d_s (mm)	E (Pa)	ν (-)	η_e (-)	
50	100	282,500 (3500)	0.16 (0.03)	0.034 (0.006)	
53	100	165,000 (7100)	0.29 (0.06)	0.062 (0.004)	
56	100	222,500 (81000)	0.29 (0.05)	0.038 (0.004)	
59	100	250,000 (0)	0.19 (0.01)	0.035 (0.021)	
59	29	3,625,000 (531000)	0.16 (0.05)	0.167 (0.096)	
64	29	4,400,000 (565000)	0.15 (0.06)	0.16 (0.014)	

flow resistivity and the viscous characteristic length to the material characterization results. To enhance prediction accuracy, the viscous characteristic length is additionally fitted using the equation:

$$\Lambda = b_1(1 - \phi)^{-b_2} \tag{10}$$

3. Results and discussion

The properties of the softwood samples under investigation are detailed in Table 1. Each sample was measured on both sides, and material characterization was performed for every individual measurement. The JCAL parameters, presented in Table 2, represent the averages (according to density categories) of all these characterizations. The sample diameter and estimated elastic properties of the samples with non-ionic surfactant are found in Table 2(b).

3.1. Incident sound absorption and density

Fig. 2 shows the average absorption curves for softwood foams foamed with SDS. As expected, the first absorption maximum shifts toward lower frequencies as the density increases. The absorption maxima are found between 1000 and 2000 Hz. The results agree with previous studies on

foam-formed softwood fibers [27,39,44]. In these earlier studies, absorption performance and flow resistivity of softwood fibers were also compared with hardwood fibers. As a result, hardwood fibers showed improved absorption properties due to higher flow resistivity. The improved flow resistivity is again caused by shorter fibers and therefore a higher fiber per volume count. However, during this study hardwood pulp was not available from the supplier and will therefore be part of future studies. Further, the absorption curves of the material with non-ionic surfactant and densities up to 64 kg/m³ are found in Fig. 3. Due to tight fitting in the impedance tube, resulting in notable elastic effects, these samples have been investigated using the JCAL-Biot model.

3.2. JCAL and JCA

Figs. 4(a)–4c illustrate the measured and modeled sound absorption curves for the three average densities of the 14 softwood samples with SDS surfactant. Figs. 4(d)–4g show the results for the samples with non-ionic surfactant and 100 mm sample diameter and Figs. 4(h)–4i are based on the samples with a 29 mm diameter. Across all samples, the absorption curves generated by the JCAL model provide the most precise results, while the JCA model also yields good outcomes across the measured frequency range. The non-acoustic parameters listed in

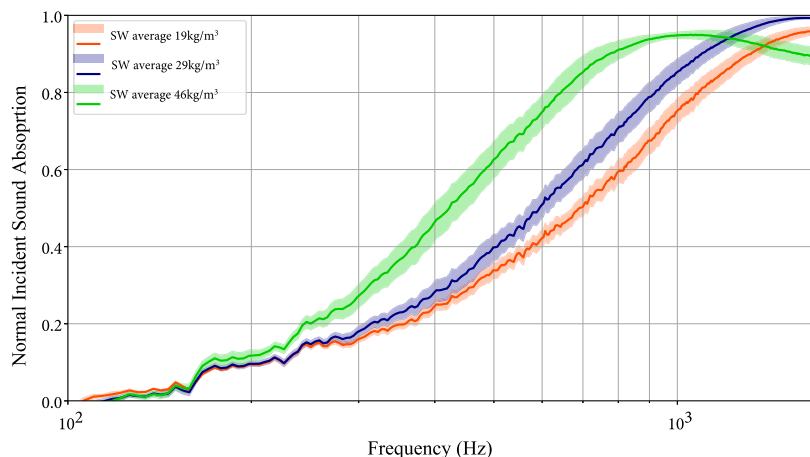


Fig. 2. Measured average absorption curves for foam-formed softwood fibers at densities 19, 29, 46 kg/m³.

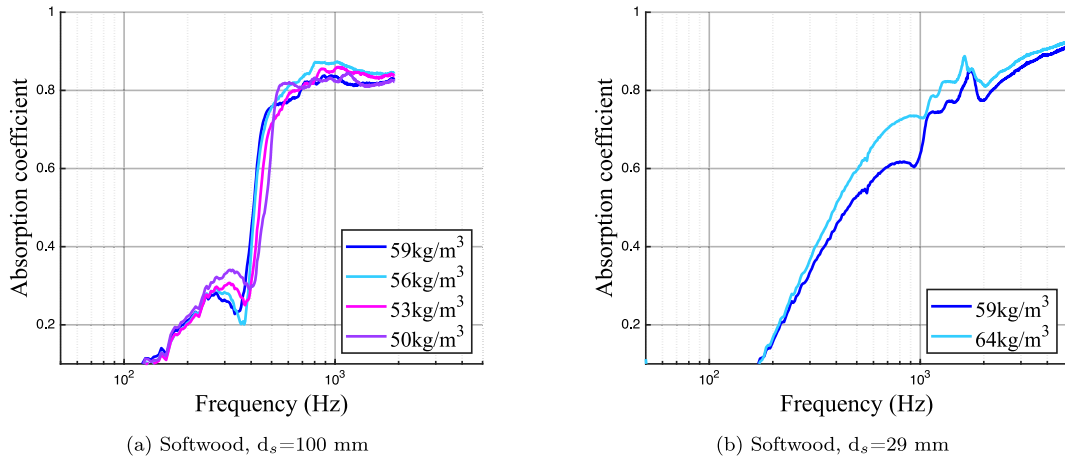


Fig. 3. Measured absorption curves for foam formed softwood fibers with non-ionic surfactant for (a) a sample diameter of 100 mm and (b) a sample diameter of 29 mm. The smaller sample diameter allows a higher frequency range, while the bigger sample diameter allows a higher accuracy at lower frequencies.

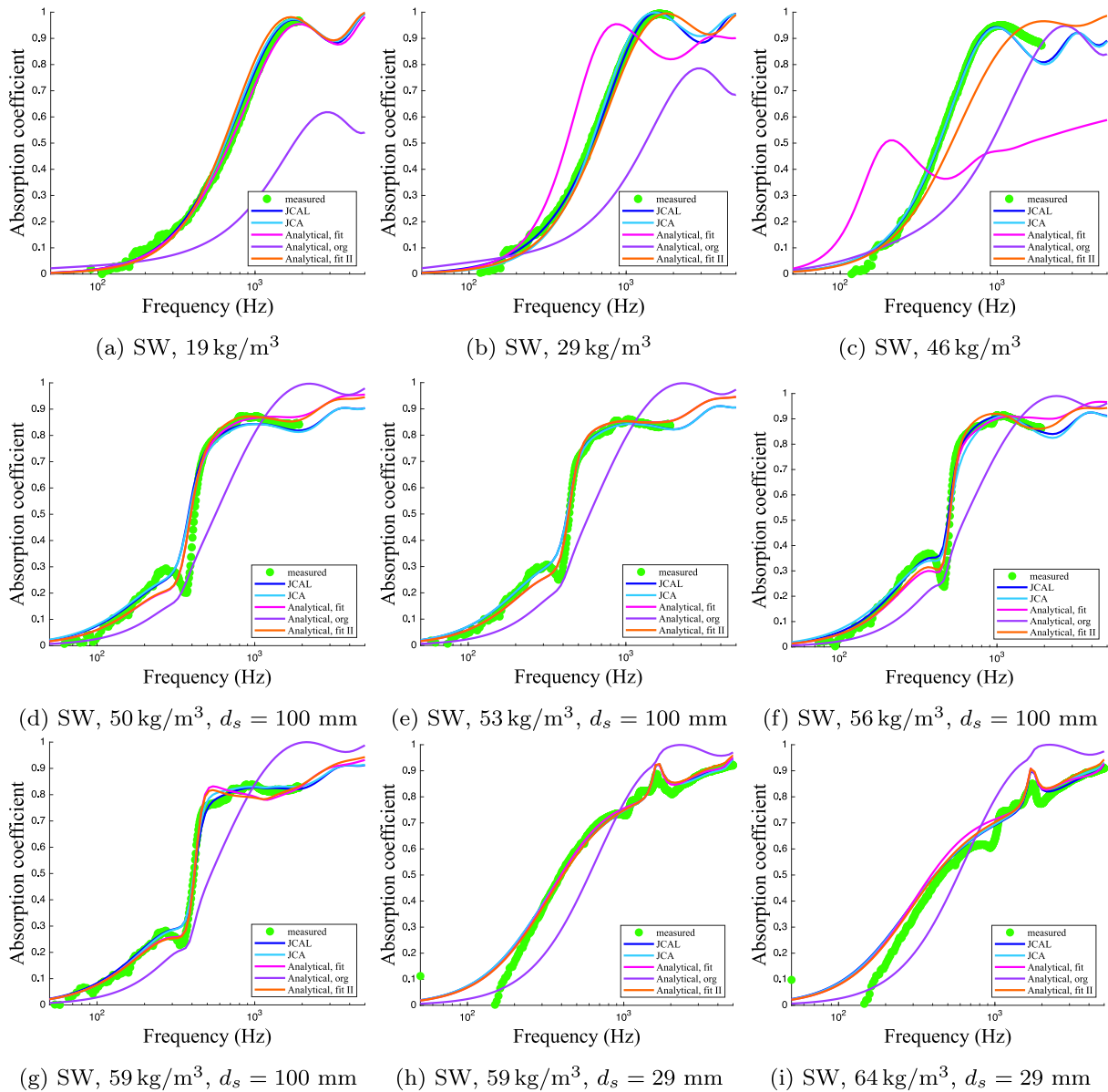


Fig. 4. Sound absorption measurements and predictions for softwood foam-formed samples from 19 to 64 kg/m³ with two diameters ($d_s = 100$ mm (a – f) and $d_s = 29$ mm (h,i)). Shown are the predicted absorption curves based on the JCAL and JCA model, as well as an original and fitted analytical model (org, fit), that has been further improved for lower densities by replacing the viscous characteristic length submodel (fit II).

Table 2 indicate that for the samples with SDS surfactant the flow resistivity increases from 5900 to 19,600 Ns/m⁴, with a slight decrease in porosity. Tortuosity is more or less constant around 1.04–1.05. The viscous characteristic length, thermal characteristic length, and thermal permeability show a decrease across densities (19–46 kg/m³). For the density range of 50–59 kg/m³ with the addition of non-ionic surfactant, the flow resistivity increases further from 37,600 to 50,400 Ns/m⁴. Porosity remains unchanged, while the tortuosity is slightly higher than in the samples with SDS surfactant. Viscous characteristic length remains stable around 22–25 μm, while the thermal characteristic length decreases from 247–146 μm. Thermal permeability slightly increases over this density range. The 29 mm samples further increase in airflow resistivity up to 73,200 Ns/m⁴ with a decrease in tortuosity, stable viscous characteristic length, and decreasing thermal characteristic length. For completeness, the estimated elastic properties are shown in Table 2(b). In future studies, these can be compared to experimentally obtained parameters which go beyond this work’s scale. However, the estimated elastic properties provide a reasonable prediction of the elastic modulation of the absorption curve. Especially, the 29 mm samples are well described by the JCAL-Biot model, while some 100 mm samples, e.g. Fig. 4(d), are not accurate in the upper half of the absorption curve at 500–2000 Hz or around the lower frequencies at 200–400 Hz.

3.3. Analytical models and parameter fitting

This study employs three analytical models to predict the sound absorption curves of foam-formed softwood fibers, all based on the framework described in [45]. Initially, the original parameters validated for parallel fibers with symmetric radius distributions in [45] are used. Further, the model and its six sub-models allow empirical fitting of variable parameters to adapt to fibrous structures that deviate from the base model and its parallel non-overlapping fiber geometry assumption. Therefore, randomly oriented fibers can also be accurately predicted to a certain extent.

Without fitting, the predicted first absorption maxima in this study are shifted towards higher frequencies across all densities compared to the measured absorption curve (see Fig. 4, ‘Analytical, org’ - violet curve). Therefore, the variables of Eq. (5) and (7) for airflow resistivity and viscous characteristic length were fitted to the values obtained from the characterization. The results show that seven of nine absorption curve predictions were close to the accuracy of the JCAL model after the analytical model has been fitted to the characterized values of flow resistivity and viscous characteristic length. The viscous characteristic length primarily influences the location of the first maximum, while

Table 3
Fitted and original values for coefficients c_1 , c_2 , exponent b , and additional model parameters b_1 and b_2 for softwood samples treated with different surfactants.

Model	c_1	c_2	b	b_1	b_2
Original model	0.7	0.2	2.732	–	–
Softwood (SDS surfactant)	1.02	0.07	149.3	4.60×10^{-7}	1.14
Softwood (non-ionic surfactant)	0.14	1.13	51.2	2.36×10^{-4}	-0.69

flow resistivity impacts the maximum absorption. Consequently, precise fitting of these parameters is crucial. However, for densities of 29 and 46 kg/m³ of the SDS softwood fibers the fitted model leads to absorption maxima shifted to lower frequencies (see Figs. 4(b), 4b, Analytical, fit - pink curve). In this case, the limits of the base model are reached and another submodel needs to be used to achieve accuracy. After fitting an exponential interpolation (Eq. (10)) to the viscous characteristic length, the model yields an accuracy close to that of the JCAL model (see Figs. 4(b), 4b, Analytical, fit II - orange curve). For the remaining samples this further step did not improve prediction accuracy.

The limits of the base model for viscous characteristic length were reached because the foam-formed softwood fibers exhibit much smaller viscous characteristic lengths than the geometry anticipated in the base model (see Fig. 5(b)). In foam-formed softwood fiber networks, the smallest dimensions affecting the viscous characteristic length arise from overlapping fibers, forming narrow voids where fibers intersect. These overlaps occur at various densities and contribute to smaller viscous lengths than predicted by the analytical model, which assumes parallel fibers without overlaps. Therefore, the minimum dimension does not change strongly with increasing material density for the investigated density range. Fig. 5(b), and Table 3 show that very high fitting parameters are needed to adjust the model to the low viscous characteristic lengths of the material. The slightly underestimated values at 29 and 46 kg/m³ emphasize how sensitive the prediction accuracy is to not optimally fitted values. In Fig. 5(a), the characterized and predicted air flow resistivity values are shown. Here, the base model assumes smaller air flow resistivities than in the investigated material. The parameter c_1 is an overall scaling factor for the resistivity expression, c_2 controls the sensitivity of changes in flow resistivity over changes in density. In this case, the SDS infused foam-formed softwood fibers exhibit higher c_1 and lower c_2 fitting values, while the non-ionic surfactant leads to lower c_1 and higher c_2 values. The stirring during the foam-forming process results in randomly oriented fibers, creating a tightly woven network that increases air flow resistivity compared to parallel fibers

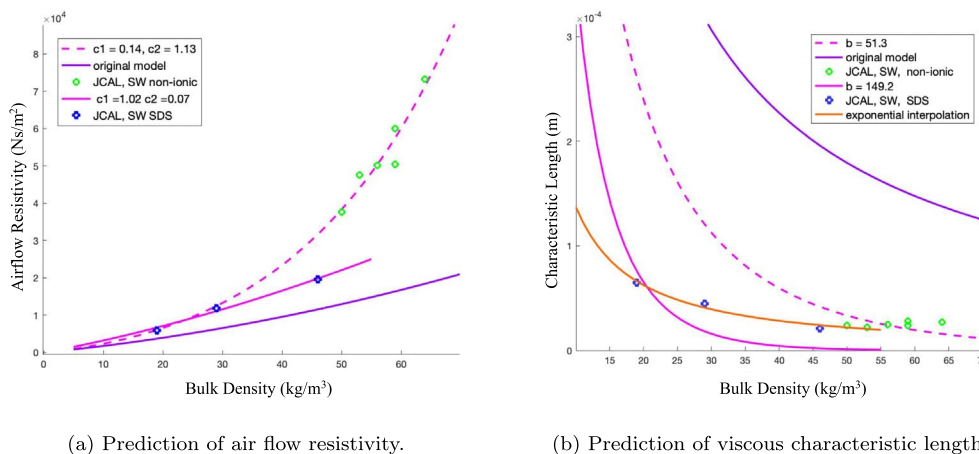


Fig. 5. Experimental, analytical, and improved analytical values for (a) flow resistivity and (b) viscous characteristic length. Here, the characterized JCAL values for the two different surfactant types are the base to which the original analytical model can be fitted. Exponential interpolation offers an alternative if the fitting is not accurate enough.

Table 4
Overview of (a) estimated JCAL parameters and (b) fitted model parameters after slight compression of the higher density samples with 100 mm sample diameter.

(a) Acoustic and structural parameters estimated in RokCell.						
Density (kg/m ³)	σ (Nsm ⁻⁴)	ϕ (-)	α_∞ (-)	Λ (μ m)	Λ' (μ m)	k'0 (1e-10 m ²)
50	23,600 (1300)	0.97	1.23 (0.13)	22 (2)	114 (11)	10 (1)
51	24,850 (1400)	0.97	1.14 (0.11)	20 (1)	100 (86)	11 (2)
53	26,600 (1100)	0.97	1.25 (0.10)	21 (4)	112 (49)	12 (5)
55	31,400 (800)	0.97	1.14 (0.18)	22 (8)	104 (79)	12 (5)
58	25,400 (2900)	0.97	1.22 (0.13)	16 (2)	107 (25)	12 (2)

(b) Fitted and original values for coefficients c_1 , c_2 , exponent b , and additional parameters b_1 , b_2 for the softwood (non-ionic, compressed) model.	
Parameter	Value
c_1	8.44×10^6
c_2	4.43×10^{-6}
b	61.64
b_1	1.59×10^{-7}
b_2	1.45

(Fig. 1(b)). Non-ionic surfactants stabilize the fiber networks and can therefore achieve higher densities without collapsing. The systematic underestimation of the viscous characteristic length Λ by the base analytical model can be attributed to its simplified geometric assumptions. The model considers parallel, non-overlapping fibers with a symmetric radius distribution, whereas the foam-formed networks investigated here exhibit random orientation, fiber overlap, and variable local pore sizes. These features lead to smaller effective viscous pathways and, consequently, lower Λ values than those predicted analytically.

While the empirical fitting of Λ improved prediction accuracy, this approach remains limited in its ability to capture the influence of local

microstructural irregularities. Future work could therefore benefit from adopting alternative frameworks that couple analytical and numerical descriptions. For example, hybrid analytical–numerical models could combine closed-form equations for macroscopic parameters with numerically resolved local flow fields (e.g., using finite element or lattice Boltzmann simulations) to account for the effects of fiber intersections and random pore geometry. Similarly, stochastic fiber network models could statistically represent the spatial distribution, orientation, and connectivity of fibers, thereby capturing the variability inherent to foam-formed structures.

Integrating such approaches would allow more physically grounded estimation of characteristic lengths and transport parameters, bridging the gap between idealized analytical models and the complex morphology of real bio-based fiber networks.

3.4. Impact of sample fitting in measurement setup

To further understand the prediction trustworthiness, we conducted an additional measurement of slightly compressed samples (horizontal plane) of densities 51–58 kg/m³ to decrease the diameter and investigate therefore a more ‘loose’ fit in the impedance tube. The aim was to reduce the impact of the solid structure elasticity and model solely the absorption in the air inside the porous network. Table 4 shows the characterized JCAL parameters as well as the analytical model fitting values. Fig. 6 shows the measured and predicted absorption curves. We can observe that the elastic resonances in the absorption curve vanished while the flow resistivity is significantly decreased in comparison to the uncompressed samples with ‘tighter’ fit in Table 2. A possible explanation is the leakage of airflow at the border of the sample and tube wall. This showcases the importance of consistent sample fitting in the impedance tube finding the balance between the presence of elastic resonances in the absorption curve and lower airflow resistivity due to leakage. The

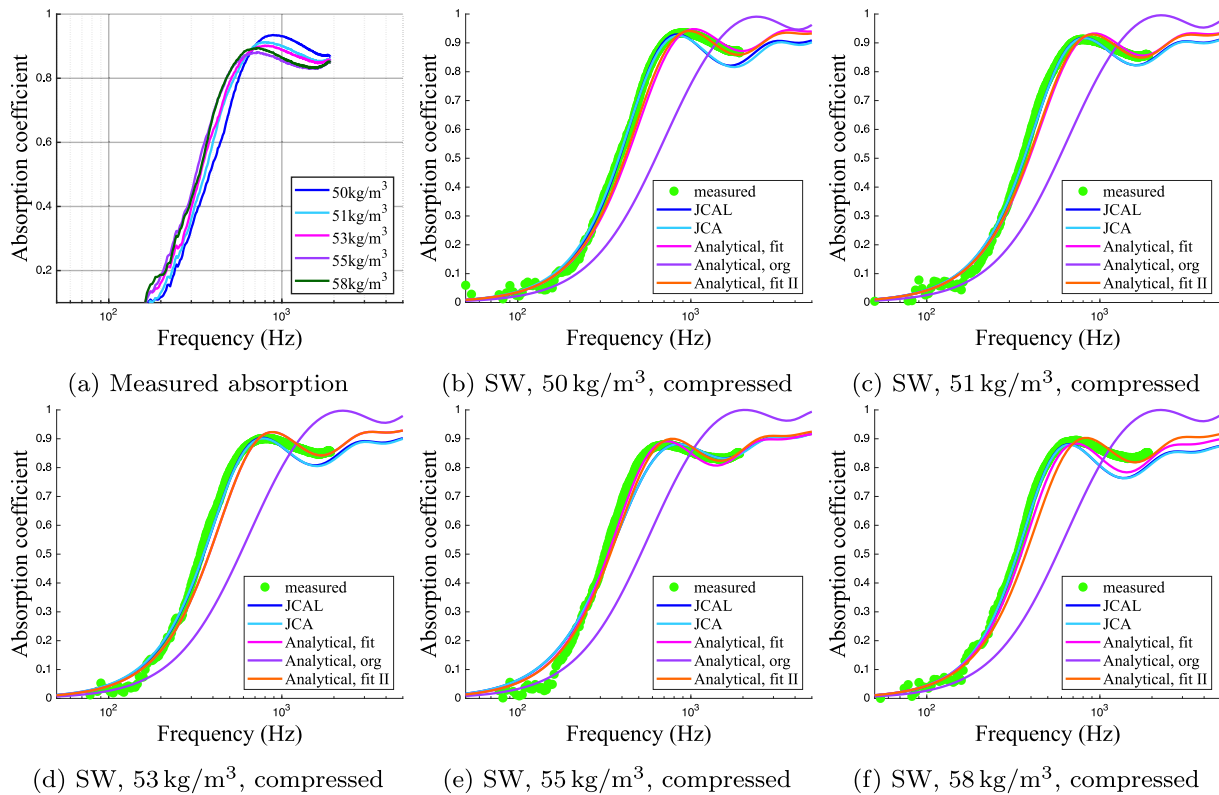


Fig. 6. Sound absorption measurements (a) and predictions (b–f) of softwood foam-formed samples from 50 to 58 kg/m³ with sample diameter $d_s = 100$ mm that have been slightly compressed to improve the fitting in the impedance tube. Shown are the predicted absorption curves based on the JCAL and JCA model, an original and fitted analytical model (org, fit), as well as an alternative viscous characteristic length submodel (fit II).

prediction results show similar accuracy like the previous samples where the JCAL model is the most accurate. The analytical model curves show a slight shift towards higher frequencies which can be related to the decrease of airflow resistivity for the last sample of density 58 kg/m^3 . This inconsistency with the expected increase of flow resistivity with increasing density is also reflected by the extreme fitting values c_1 and c_2 for the flow resistivity seen in Table 3. Further, it needs to be acknowledged that the absorption performance of foam-formed softwood fibers depends on how tightly the material is fitted into its surrounding environment. Additionally, the estimated mechanical properties are also dependent on the sample fitting in the tube and do not replace a conventional experimental characterization which is the objective of future studies.

4. Conclusion

In this study, 14 samples of foam-formed softwood with SDS surfactant and 6 samples with non-ionic surfactant were produced, and their normal incidence sound absorption was assessed. Based on these measurements, non-acoustic parameter characterizations were conducted and utilized as inputs for the JCAL and JCA models as well as taking into account the elastic parameters of the Biot model. An analytical model for parallel natural fibers was refined to enhance the accuracy of predicted sound absorption curves. For those samples that could not achieve accurate prediction results, the viscous characteristic length was fitted to an exponential interpolation, increasing overall accuracy.

This work establishes a foundation in characterizing, modeling and predicting sound absorption in foam-formed wood fibers made from bleached softwood. Ultimately, our goal is to create environmentally sustainable sound absorbers with precisely tailored absorption properties for desired frequency ranges. Future research should focus on investigating the accuracy of the estimated elastic properties and the effect of material compression as well as extending predictions to other pulp types, such as hardwood pulp, which may offer better sound absorption due to smaller fiber dimensions and a greater number of fibers per volume.

CRediT authorship contribution statement

Janis Heldmann: Writing – review & editing, Writing – original draft, Visualization, Validation, Software, Methodology, Investigation, Funding acquisition, Formal analysis, Data curation, Conceptualization. **Jose Cucharero:** Resources. **Tapio Lokki:** Writing – review & editing, Validation, Supervision, Project administration, Investigation, Funding acquisition.

Declaration of competing interest

The authors declare the following financial interests/personal relationships which may be considered as potential competing interests:

Janis Heldmann reports that financial support was provided by the KAUTE Foundation. Janis Heldmann also reports that financial support was provided by the Academy of Finland. If there are other authors, they declare that they have no known competing financial interests or personal relationships that could have appeared to influence the work reported in this paper.

Acknowledgements

This work was supported by the KAUTE Foundation and the Academy of Finland's Flagship Programme under Projects No. 318890 and 318891 (Competence Center for Materials Bioeconomy, FinnCERES).

References

- [1] Bujoreanu C, Nedeff F, Benchea M, Agop M. Experimental and theoretical considerations on sound absorption performance of waste materials including the effect of backing plates. *Appl Acoust* 2017;119:88–93. <https://doi.org/10.1016/j.apacoust.2016.12.010>
- [2] Klatt M, Hellbrück J, Seidel J, Leistner P. Effects of classroom Acoustics on performance and well-being in elementary school children: a field study. *Environ Behav* 2010;42(5):659–92. <https://doi.org/10.1177/0013916509336813>
- [3] Shield BM, Dockrell JE. The effects of noise on children at school: a review. *Build Acoust* 2003;10:97–116. <https://doi.org/10.1260/135101003768965960>
- [4] Durap N, Shield BM, Dance S, Sullivan R, Gomez-Agustina L. How classroom Acoustics affect the vocal load of teachers. In: *Energy Procedia*, vol. 78. 2015. pp. 3084–9. <https://doi.org/10.1016/j.egypro.2015.11.761>
- [5] Tiesler G, Oberdörster M. Noise — a stressor? acoustic ergonomics of schools. *Build Acoust* 2008;15(3):249–61. <https://doi.org/10.1260/135101008786348690>
- [6] Haapakangas A, Hongisto V, Hyönä J, Kokko J, Keränen J. Effects of unattended speech on performance and subjective distraction: the role of acoustic design in open-plan offices. *Appl Acoust* 2014;86:1–16. <https://doi.org/10.1016/j.apacoust.2014.04.018>
- [7] Hongisto V, Haapakangas A, Varjo J, Helenius R, Koskela H. Refurbishment of an open-plan office – environmental and job satisfaction. *J Environ Psychol* 2016;45:176–91. <https://doi.org/10.1016/j.jenvp.2015.12.004>
- [8] Steffens J, Wilczek T, Weinzierl S. Junk food or Haute cuisine to the ear? – investigating the relationship between room acoustics, soundscape, non-acoustical factors, and the perceived quality of restaurants. *Frontiers in Built Environment* 2021;7:676009. <https://doi.org/10.3389/fbuil.2021.676009>
- [9] Yu T, Jiang F, Zhang R, Cao M, Qin R, Guo C, Wang Z, Chang Y. Effects of volume fraction and diameter of hollow spheres on acoustic properties of metallic-hollow-sphere/polyurethane (MHSP) acoustic composites. *Composite Structures* 2021;261:113554. <https://doi.org/10.1016/j.compstruct.2021.113554>
- [10] Tang X, Yan X. Acoustic energy absorption properties of fibrous materials: a review. *Compos Part A Appl Sci Manuf* 2017;101:360–80. <https://doi.org/10.1016/j.compositesa.2017.07.002>
- [11] Cao L, Shan H, Zong D, Yu X, Yin X, Si Y, Yu J, Ding B. Fire-resistant and hierarchically structured elastic ceramic nanofibrous aerogels for efficient low-frequency noise reduction. *Nano Lett* 2022;22:1609–17. <https://doi.org/10.1021/acs.nanolett.1c04532>
- [12] Arenas JP, del Rey R, Alba J, Oltra R. Sound-absorption properties of materials made of Esparto grass fibers. *Sustainability Switzerland* 2020;12:5533. <https://doi.org/10.3390/su12145533>
- [13] Ye F, Wei H, Xiao Y, Berardi U, Quaranta G, Demartino C. Bio-based insulation materials in sustainable constructions: a review of environmental, thermal and acoustic insulation, durability, and mechanical performances. *Renew Sustain Energy Rev* 2025;223:115872. <https://doi.org/10.1016/j.rser.2025.115872>
- [14] Korjakins A, Sahmenko G, Lapkovskis V. A short review of recent innovations in acoustic materials and panel design: emphasizing wood composites for enhanced performance and sustainability. *Appl Sci* 2025;15:4644. <https://doi.org/10.3390/app15094644>
- [15] Taban E, Tajpoor A, Faridan M, Samaei SE, Beheshti MH. Acoustic absorption characterization and prediction of natural coir fibers. *Acoustics Australia* 2019;47:66–7. <https://doi.org/10.1007/s40857-019-00151-8>
- [16] Taban E, Khavanin A, Ohadi A, Putra A, Jafari AJ, Faridan M, Soleimani A. Study on the acoustic characteristics of natural date palm fibres: experimental and theoretical approaches. *Build Environ* 2019;161:106274. <https://doi.org/10.1016/j.buildenv.2019.106274>
- [17] Taban E, Khavanin A, Faridan M, Samaei SE, Samimi K, Rashidi R. Comparison of acoustic absorption characteristics of coir and date palm fibers: experimental and analytical study of green composites. *Int J Environ Sci Technol* 2020;17:39–48. <https://doi.org/10.1007/s13762-019-02304-8>
- [18] Taban E, Amininasab S, Soltani P, Berardi U, Abdi DD, Samaei SE. Use of date palm waste fibers as sound absorption material. *J Build Eng* 2021;41:102752. <https://doi.org/10.1016/j.jobe.2021.102752>
- [19] Berardi U, Iannace G. Predicting the sound absorption of natural materials: best-fit inverse laws for the acoustic impedance and the propagation constant. *Appl Acoust* 2017;115:131–8. <https://doi.org/10.1016/j.apacoust.2016.08.012>
- [20] Taban E, Soltani P, Berardi U, Putra A, Mousavi SM, Faridan M, Samaei SE, Khavanin A. Measurement, modeling, and optimization of sound absorption performance of Kenaf fibers for building applications. *Build Environ* 2020;180:107087. <https://doi.org/10.1016/j.buildenv.2020.107087>
- [21] Soltani P, Taban E, Faridan M, Samaei SE, Amininasab S. Experimental and computational investigation of sound absorption performance of sustainable porous material: yucca gloriosa fiber. *Appl Acoust* 2020;157:106999. <https://doi.org/10.1016/j.apacoust.2019.106999>
- [22] Raj M, Fatima S, Tandon N. An experimental and theoretical study on environment-friendly sound absorber sourced from nettle fibers. *J Build Eng* 2020;31:101395. <https://doi.org/10.1016/j.jobe.2020.101395>
- [23] Muthuraj R, Lacoste C, Lacroix P, Bergeret A. Sustainable thermal insulation bio-composites from rice husk, wheat husk, wood fibers and textile waste fibers: elaboration and performances evaluation. *Ind Crops Prod* 2019;135:238–45. <https://doi.org/10.1016/j.indcrop.2019.04.053>
- [24] Aly NM, Seddeq HS, Elnagar K, Hamouda T. Acoustic and thermal performance of sustainable fiber reinforced thermoplastic composite panels for insulation in buildings. *J Build Eng* 2021;40:102747. <https://doi.org/10.1016/j.jobe.2021.102747>
- [25] Maderuelo-Sanz R, Acedo-Fuentes P, García-Cobos FJ, Sánchez-Delgado FJ, Mota-López MI, Meneses-Rodríguez JM. The recycling of surgical face masks as sound porous absorbers: preliminary evaluation. *Sci Total Environ* 2021;786:147461. <https://doi.org/10.1016/j.scitotenv.2021.147461>
- [26] Maderuelo-Sanz R. Characterizing and modelling the sound absorption of the cellulose acetate fibers coming from cigarette butts. *J Environ Health Sci Eng* 2021;19:1075–86. <https://doi.org/10.1007/s40201-021-00675-0>

- [27] Cucharero J, Ceccherini S, Maloney T, Lokki T, Hänninen T. Sound absorption properties of wood-based pulp fibre foams. *Cellulose* 2021;28:4267–79. <https://doi.org/10.1007/s10570-021-03774-1>
- [28] Lipiäinen S, Kuparinen K, Sermyagina E, Vakkilainen E. Pulp and paper industry in energy transition: towards energy-efficient and low carbon operation in Finland and Sweden. *Sustain Prod Consum* 2022;29:421–31. <https://doi.org/10.1016/j.spc.2021.10.029>
- [29] Chambers JQ, Higuchi N, Tribuzy ES, Trumbore SE. Carbon sink for a century. *Nature* 2001;410:429. <https://doi.org/10.1038/35068624>
- [30] Lumir Oy. Environmental product declaration; 2024. https://lumir.fi/wp-content/uploads/2024/07/rts_162_21-one-click-lca-lumir-epd_20211208.pdf [accessed: 23 Oct 2025].
- [31] Lashgari M, Taban E, SheikhMozafar MJ, Soltan P, Attenborough K, Khavanin A. Wood chip sound absorbers: measurements and models. *Appl Acoust* 2024;220:109963. <https://doi.org/10.1016/j.apacoust.2024.109963>
- [32] Valkonen MJ, Cucharero J, Lokki T, Rautkari L, Hänninen T. Preparation of fully bio-based sound absorbers from waste wood and pulp fibers by foam forming. *BioResources* 2023;18:2657–69. <https://doi.org/10.15376/biores.18.2.2657-2669>
- [33] Delany ME, Bazley EN. Acoustical properties of fibrous absorbent materials. *Appl Acoust* 1970;3(2):105–16. [https://doi.org/10.1016/0003-682X\(70\)90031-9](https://doi.org/10.1016/0003-682X(70)90031-9)
- [34] Jaouen L, Gourdon E, Glé P. Estimation of all six parameters of Johnson-Champoux-Allard-Lafarge model for acoustical porous materials from impedance tube measurements. *J Acoust Soc Am* 2020;148(4):1998–2005. <https://doi.org/10.1121/10.0002162>
- [35] Kalle H, Joulain K. Design and thermal conductivity of 3d artificial cross-linked random fiber networks. *Mater Des* 2022;220:110800. <https://doi.org/10.1016/j.matdes.2022.110800>
- [36] Pompoli F. Acoustical characterization and modeling of sustainable posidonia fibers. *Applied Sciences Switzerland* 2023;13(7):4562. <https://doi.org/10.3390/app13074562>
- [37] Pöhler T, Jetsu P, Isoimoisio H. Benchmarking new wood fibre-based sound absorbing material made with a foam-forming technique. *Build Acoust* 2016;23(3–4):131–43. <https://doi.org/10.1177/1351010X16661564>
- [38] International Organization for Standardization. ISO 10534-2:1998 Acoustics – determination of sound absorption coefficient and impedance in impedance tubes – part 2: transfer-function method, Tech. rep., Geneva, Switzerland: ISO; 1998 [accessed: 23 Oct 2025].
- [39] Cucharero J, Ceccherini S, Awais M, Kammiovirta K, Maloney T, Rautkari L, Lokki T, Hänninen T. Studies on the sound absorption properties of wood-based pulp fibre foams. In: *Proceedings of the International Congress on Acoustics*. Gyeongju, Korea: International Commission for Acoustics; 2022.
- [40] Tamayol A, Bahrami M. Transverse permeability of fibrous porous media. *Phys Rev E Stat Nonlinear Soft Matter Phys* 2011;83(4):046314. <https://doi.org/10.1103/PhysRevE.83.046314>
- [41] Allard JF, Atalla N. Propagation of sound in porous media. 2nd ed. Chichester, UK: John Wiley & Sons; 2009. <https://doi.org/10.1002/9780470747339.fmatter>
- [42] Umnova O, Tsiklauri D, Venegas R. Effect of boundary slip on the acoustical properties of microfibrinous materials. *J Acoust Soc Am* 2009;126(4):1850–61. <https://doi.org/10.1121/1.3204087>
- [43] Luu HT, Panneton R, Perrot C. Effective fiber diameter for modeling the acoustic properties of polydisperse fiber networks. *J Acoust Soc Am* 2017;141(2):96–101. <https://doi.org/10.1121/1.4976114>
- [44] Cucharero J, Awais M, Valkonen M, Kammiovirta K, Rautkari L, Lokki T, Hänninen T. Influence of moisture on the sound absorption properties of wood-based pulp fibre foams. *Materials Today Sustainability* 2024;27:100854. <https://doi.org/10.1016/j.mtsust.2024.100854>
- [45] Pompoli F, Bonfiglio P. Definition of analytical models of non-acoustical parameters for randomly-assembled symmetric and asymmetric radii distribution in parallel fiber structures. *Appl Acoust* 2020;159:107091. <https://doi.org/10.1016/j.apacoust.2019.107091>